Design of High-power AC Motor Controllers using Sine Wave Pulse Width Modulation

Guo-Shing Huang, *Senior Member, IEEE*, Hsiung-Cheng Lin, Yu-Yong Tseng

***Abstract*—General power system supply only provides a fixed voltage and frequency, and its the inverter is mostly used to control AC motor speed with different frequencies. However, it normally requires a rectified DC into AC for the frequency variation. In this study, a digital signal processing technology is developed to generate a Sine Wave Pulse Width Modulation (SPWM) signal to replace the traditional inverter design. Accordingly, the proposed inverter switching signals generated from SPWM can control brushless AC servo motor more easily and accurately. Both simulation and experimental results are proved to verify the effectiveness of the proposed scheme.**

***Index Terms*—**Brushless-AC-servo-motor, SPWM, encoder, feedback-position-signal, inverter

I. Introduction

With the rapid development of power electronics technology in microelectronics, new motor control theory and permanent magnet materials, now AC servo motor control in industry has become a major discipline. As a result, the precision positioning, speed control or current control in AC servo motor are required for a high performance quality following up the current industrial trend. In this paper, the permanent AC servo motor is studied.

It is well known that the brushless AC motor is very popular due to simple structure, no carbon brushes and commutation segment. Also, it does not generate friction, dust and sparks, also having an advantage like DC motor performance. Brushless AC motor using electronic commutation circuit can replace the traditional brush motor using brush commutation mechanism, but requiring a motor driver to operate [1]-[5]. The Hall element can be used to detect the position of rotator so that the mechanical noise and maintenance cost can be reduced, thus extending its working life. Another advantage is that its phase commutation time can be accurately calculated using a position feedback control circuit.

In addition, a linear relation between the output torque and motor current can be made using a suitable power electronic driver, i.e. the output torque equals to the constant multiplying input current [6][7]. It provides a high torque at low speed. Consequently, it has been widely applied in electric vehicles [8]-[12].

This paper is organized as follows, Section II depicts the system architecture of brushless AC three-phase motor. Section III describes the control model of sine wave width modulation drive. The analysis and discussion of experimental results are shown in section IV. Section V makes some conclusions and gives recommendations for future work.

Manuscript received March 5, 2014; revised April 3, 2014. This work was supported by the National Science Council of Taiwan R.O.C. under grant NSC101-2221-E-167-020-MY2.

Guo-Shing Huang, is with Department of Electronic Engineering, National Chin-Yi University of Technology, Taichung 41170, Taiwan (corresponding author phone: 886-4-23924505-7338; fax: 886-4-23926610; e-mail: hgs@ncut.edu.tw).

Hsiung-Cheng Lin, is with Department of Electronic Engineering, National Chin-Yi University of Technology, Taichung 41170, Taiwan (e-mail: hclin@ncut.edu.tw).

Yu-Yong Tseng, is with Department of Electronic Engineering, National Chin-Yi University of Technology, Taichung 41170, Taiwan (e-mail: happy62196227@yahoo.com.tw).

II. System Architecture

A. Brushless AC motor structure

Typically, the motor can be classified into carbon brush and brushless motors. The motor with carbon brush is the DC motor, and the permanent magnet is fixed on the stator. The rotor (armature) that can rotate consists of winding and the core, where torque is produced by flowing current. For brushless AC motor, the rotor is a permanent magnet and its windings (armature) is assembled on the stator. In Figure 1, it can be seen that the brushless motor excitation is constituted by the permanent magnet on the rotor, and the armature is located in the stator. Therefore, it does not need brush to conduct current. Generally, according to stator winding classification, brushless AC motor has two-phase, three-phase, and five-phase. The three-phase brushless AC motor is most common in industry.

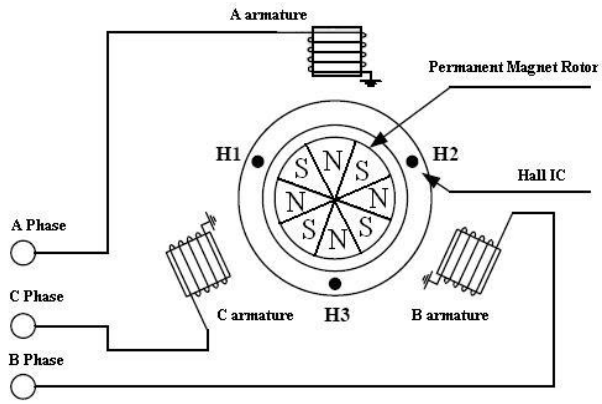

Figure 1. BLDC structure.

B. Three-phase Brushless AC motor driver

The driver circuit is required to drive the three-phase brushless AC motor. This can be done using three wired line, where sine wave signal input from three coils is the synthesis of a rotating magnetic field to rotate the rotor. The Hall IC can be used to sense the rotor pole, and the position angle of

ISBN: 978-988-19252-7-5
ISSN: 2078-0958 (Print); ISSN: 2078-0966 (Online)

the permanent magnet can be thus obtained. Then, the order of the excitation signal can be determined.

The primary drive line is shown in Figure 2. We know that the power electronics inverter normally consists of six IGBT (gate bipolar transistor, Insulated Gate Bipolar Transistor) switch for switching the operation to control Q1 to Q6.

The controller software uses Microchip's 16-bit dsPIC30F4011 digital signal controller, where it has a 10-bit, 500 KSPS analog-to-digital converters, motor control pulse width modulation module, positioning encoders and other modules interface.

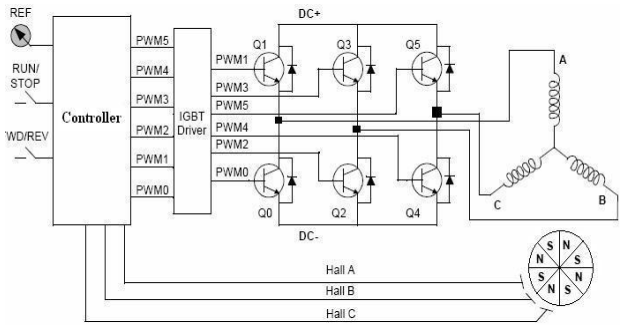

Figure 2. BLDC motor drive circuit.

The controller hardware (YBL9D-130L) of brushless AC three-phase motor we used is produced by Wild Electromechanical Industry Co., Ltd. In Figure 3 (a), the required power supply is 110 ~ 220V, and its rated speed is about 2000rpm with instant maximum torque 119Kg-cm. The driver control panel is shown in Figure 3 (b), containing AC-DC converter circuit, current sensing circuit, over-voltage and over-current protections detection circuit, low electric-current low-voltage protection detection circuit, brake circuit isolation circuit, inverter circuit and other circuits.

Figure 3. Entity diagram (a) YBL9D-130L (b) drive control panel.

C. Feedback system of three-phase brushless AC motor

In this study, we used three-phase brushless AC motor with incremental encoder and 2500 pulses / revolution. A and B signals phase which has 90 degree difference between each signal can be used to determine the motor turning direction, the position of the motor rotor, speed and other information. The Z signal (index) is generated by rotating one cycle of motor. Figure 4 indicates the starting point for every cycle. Sequentially, the angle value can be defined and used for resetting the position (angle).

Figure 5 shows the electrical current-isolated feedback circuit. This paper used an optical coupling IC (6N136) which has a light-emitting two-pole body with a sense of photoelectric crystal. The light-emitting diode can control the sense of output photoelectric crystal. In this circuit, the output current is isolated via the Hall sensor and converted into a voltage signal. Then, the signal is amplified by the inverting amplifier, where the gain can be adjusted to achieve the level available at a reasonable range.

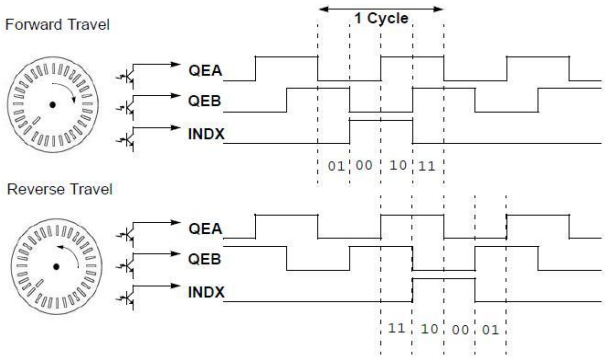

Figure 4. Incremental encoder A, B and Z output signal.

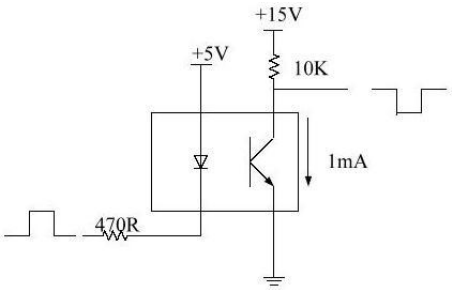

Figure 5. Current-isolated feedback circuit.

III. CONTROL MODEL OF SINE WAVE WIDTH MODULATION DRIVE

Basically, brushless motor drive may be divided into four categories: (1) Six Step Trapezoidal Control, (2) Sinusoidal Pulse-Width Modulation, (3) Space Vector Pulse-Width Modulation [13] [14], (4) Field Oriented Control [15]-[19]. The third and forth control methods require a magnetic flux sensor (current type and the voltage type) to be installed on the motor so that the magnetic flux can be accurately estimated from stator voltage and stator. However, complex mathematical model must be developed in this case. This paper used dsp30F4011 control chip to design a DSP-based SPWM control system from the rotor position signal. The SPWM waveform can be very close to a sine wave so that it can drive brushless DC motor smoothly with low noise, small torque ripple, high efficiency, and good control characteristics, etc. Particularly, the low-speed operation in the feature is obviously superior to traditional six-step square wave driving method.

A. Sinusoidal pulse width modulation

Sinusoidal pulse width modulation in the inverter is most used technology in industry [20]-[24]. Its principle is that the sinusoidal wave voltage command is generated by the controller and then compared with the triangular carrier wave.

ISBN: 978-988-19252-7-5
ISSN: 2078-0958 (Print); ISSN: 2078-0966 (Online)

Therefore, the pulse width modulation signal is thus produced. In Figure 6, the SPWM signal is generated from dsPIC30F4011 output, and the triangular wave is obtained by the PTPER and PTMR register. The pulse width modulation signal is determined by PDC1, PDC2, PDC3 registers.

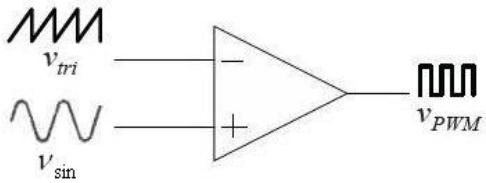

Figure 6. The SPWM wave generation schematic diagram.

In this study, the brushless servo motor has 8 poles, i.e., four pairs of poles, as shown in Figure 7. There are six different groups of the Hall signals for each electrical cycle, and for every motor rotation, Hall sensor signal will change 24 times. The Hall position signal is to determine the phase of the motor in order to drive it with the sine wave. The sensors in the motor are Hall A, Hall B and Hall C, and connected to the dsPIC30F4011 the RB0, RB1, RB2, respectively. With built-in input capture input (Change Notification CN), the Hall location signal can be obtained. Once these changes are detected, the CN interrupt is generated immediately. During one cycle, only one Hall sensor phase changes its input state for every 60 degrees. Consequently, the initial rotation amount will be provided in the beginning, and corresponding phases of Hall sensors will be also given. For this mechanism of phase adjustment, the sine wave can be sent into the motor to achieve the desired positioning.

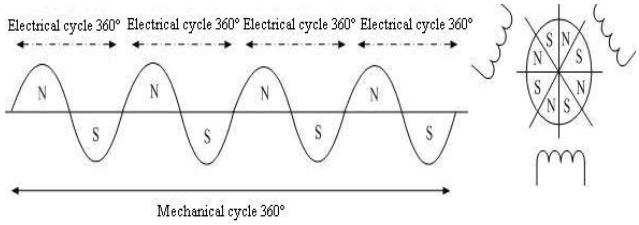

Figure 7. Eight motor electrical cycle diagram.

B. Sine wave driving method

The principle of Sine wave driving method is based on the difference between charge and discharge time in the inductance of the brushless motor. The inverter is to converter DC into a three-phase AC voltage, and switching frequency then is in accordance with the rotational speed of the motor, where the changeover timing is according to the position of the motor rotor.

As shown in Figures 8 to 10, when it is at the intersection of two waves, the switch timing occurs. The yellow solid line is the U-phase sinusoidal modulation wave; green solid line is the V-phase sinusoidal modulation wave; blue solid line is the W-phase sinusoidal modulation wave; brown solid line is a triangular cross-sectional wave; red solid line the generated voltage waveform from each phase.

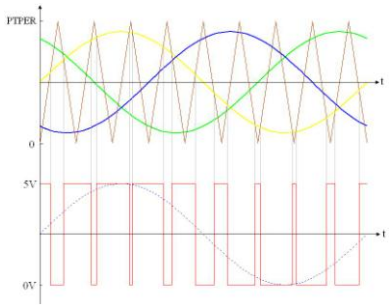

Figure 8. U-phase SPWM wave generation method diagram.

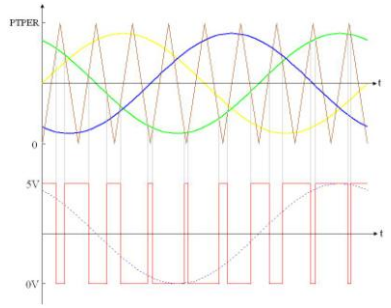

Figure 9. V-phase SPWM wave generation method diagram.

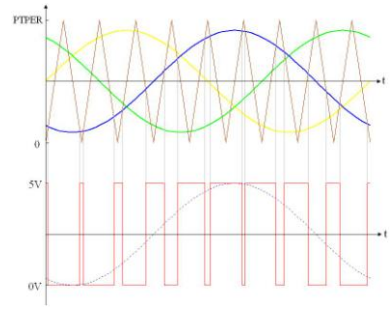

Figure 10. W-phase SPWM wave generation method diagram.

C. The establishment of a sine wave table

In this study, the brushless servo motor 8 poles with 4 pole pairs. When the motor rotates one circle, the position detector encoder generates 2500Pulse, 2500/4 = 625, 625 points. As a result, every scale has 360/625 = 0.576, i.e., a grid is set to 0.576 degrees and with the motor encoder scale. With the ROM of dsPIC30F4011, the sine wave table is stored in the program in advance. It can be called out corresponding to the correct position of the motor.

$$\text{Sintable}_N = \sin(\frac{2\pi + 2\pi * N}{625}) \qquad (0 \le N \le 624) \quad (1)$$

where Sintable_N is the N-point value sine wave.

Substitute N = 0 ~ 624 into equation (1), and sine-point value can be thus obtained under different angles.

A three-phase signal brushless servo motor has U, V, W phase. Accordingly, dsPIC30F4011 chip meter reading must be 120 degrees out of phase in the sine wave signal, divided into three intervals sine wave value to produce a rotating magnetic field alternately. As shown in Figures 11 to 13, the U phase of the conduction order is (1) (2) (3); V phase conduction sequence is (2) (3) (1); W phase of the conduction order is (3) (1) (2). This procedure continues until the stop command is issued.

ISBN: 978-988-19252-7-5
ISSN: 2078-0958 (Print); ISSN: 2078-0966 (Online)

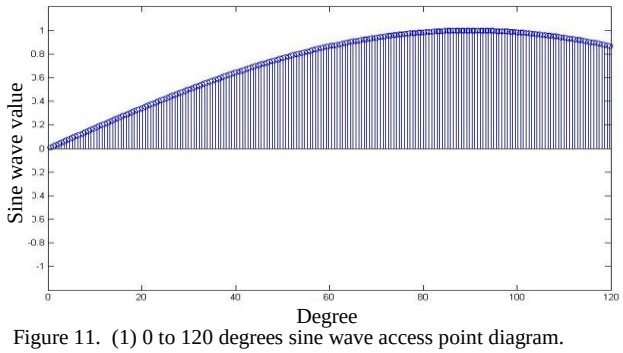

Figure 11. (1) 0 to 120 degrees sine wave access point diagram.

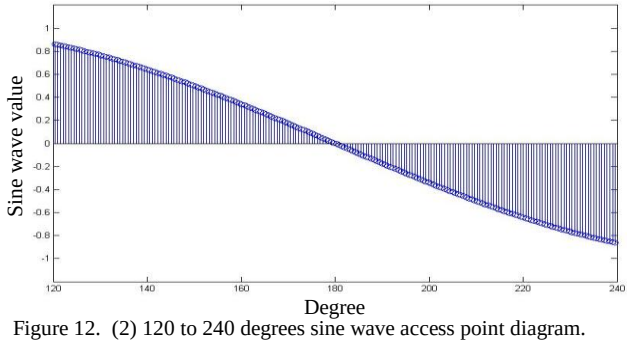

Figure 12. (2) 120 to 240 degrees sine wave access point diagram.

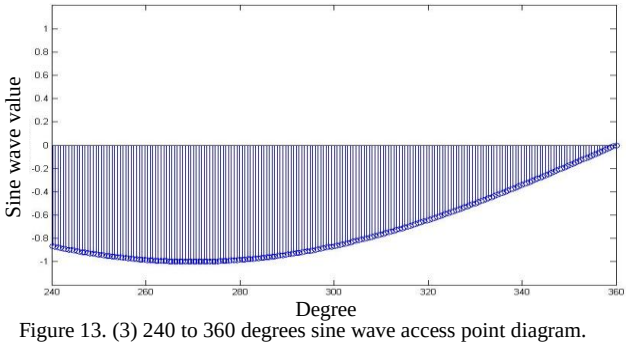

Figure 13. (3) 240 to 360 degrees sine wave access point diagram.

Unlike a six-step square wave drive that requires six of Hall sensor commutation signals to control appliances in a cycle, Sine wave inverter drive must have more detailed rotor position information to operate. In this study, the built-in encoder of position detector from AC brushless motor is used as output, providing continuous position information. Therefore, dsPIC30F4011 digital signal controller chip is used to design the interface (QEI module) to receive the position of the motor, shown in Figure 14.

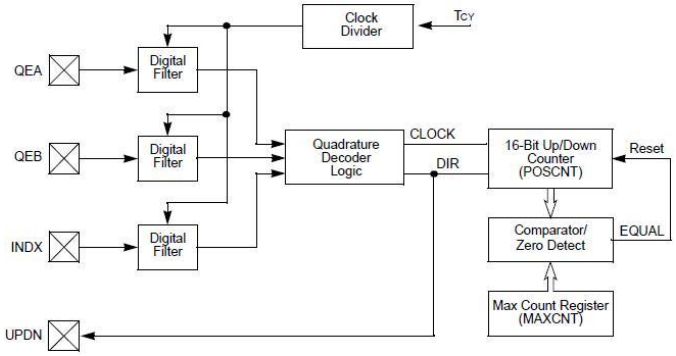

Figure 14. QEI module

D. The conduction state of the power transistor IGBT switch

There are six power transistors IGBT in the inverter circuit, forming eight states from three-pair combination. Among them, six states belong to a non-zero voltage state, and two states is a zero voltage state. The six non-zero voltage state has 60 degree adjacent plane between each other, as shown in Figure 15.

In this study, six voltage combinations are generated from eight voltage states, as shown in Figures 16 to 23, and black arrow means a current direction. Table I is the switching state of the inverter. The voltage state of "1" indicates the upper arm switching is turned on, where the lower arm is switched off. On the other hand, the "0" indicates the upper arm is switched off, and the lower arm switch is conducted.

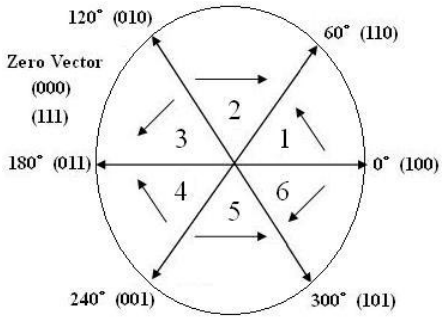

Figure 15. The eight voltage states.

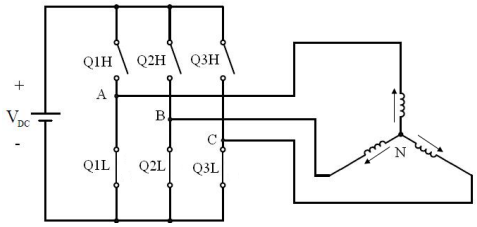

Figure 16. Power transistor conduction status at voltage state 000.

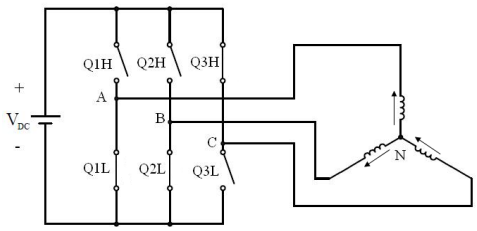

Figure 17. Power transistor conduction status at voltage state 001.

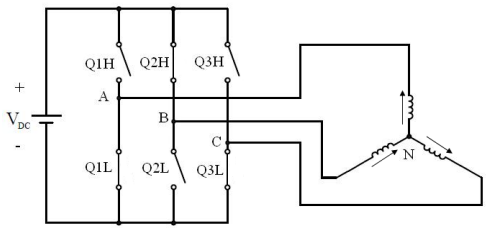

Figure 18. Power transistor conduction status at voltage state 010.

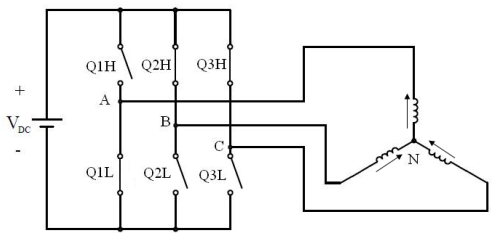

Figure 19. Power transistor conduction status at voltage state 011.

ISBN: 978-988-19252-7-5
ISSN: 2078-0958 (Print); ISSN: 2078-0966 (Online)

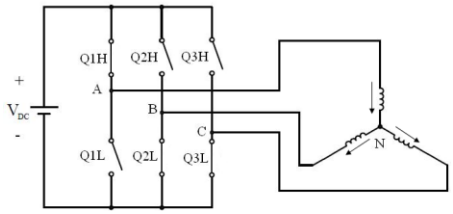

Figure 20. Power transistor conduction status at voltage state 100.

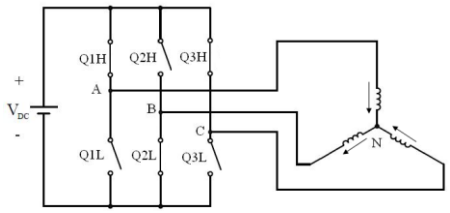

Figure 21. Power transistor conduction status at voltage state 101.

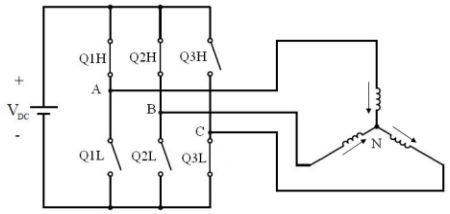

Figure 22. Power transistor conduction status at voltage state 110.

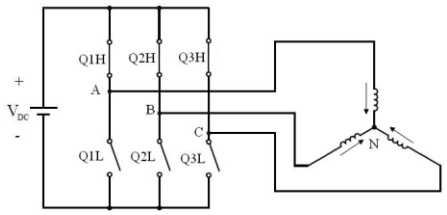

Figure 23. Power transistor conduction status at voltage state 111.

TABLE I
INVERTER SWITCHING STATE

Switch	Q_1	Q_2	Q_3	V_{AN}	V_{BN}	V_{CN}
Voltage	0	0	0	0	0	0
state	0	0	1	$2V_{DC}/3$	$-V_{DC}/3$	$-V_{DC}/3$
	0	1	0	$V_{DC}/3$	$V_{DC}/3$	$-2V_{DC}/3$
	0	1	1	$-V_{DC}/3$	$2V_{DC}/3$	$-V_{DC}/3$
	1	0	0	$-2V_{DC}/3$	$V_{DC}/3$	$V_{DC}/3$
	1	0	1	$-V_{DC}/3$	$-V_{DC}/3$	$2V_{DC}/3$
	1	1	0	$V_{DC}/3$	$-2V_{DC}/3$	$V_{DC}/3$
	1	1	1	0	0	0

E. Switch conduction change of power transistor IGBT

The forward and reversing operation in brushless servo motor is related with six voltage combinations. The change order with 1-2-3-4-5-6-1 is to rotate motor forward. To reverse the motor, just simply change the order, as shown in Figures 24 to 29. The six voltage combinations are generated by dsPIC30F4011 chip that reads the sine wave change.

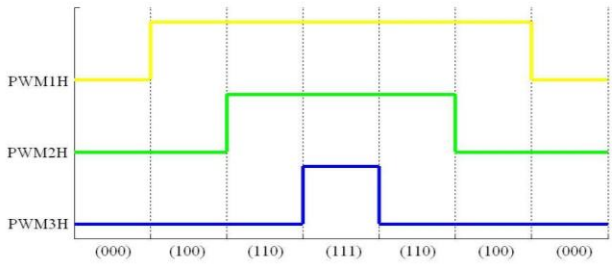

Figure 24. First changes in voltage combination.

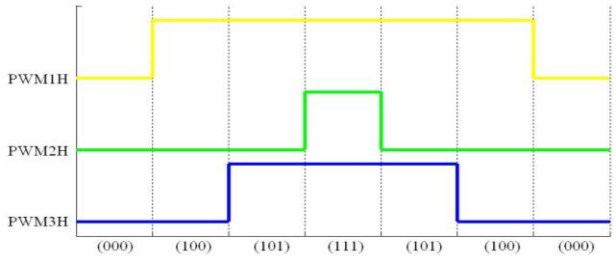

Figure 25. Second changes in voltage combination.

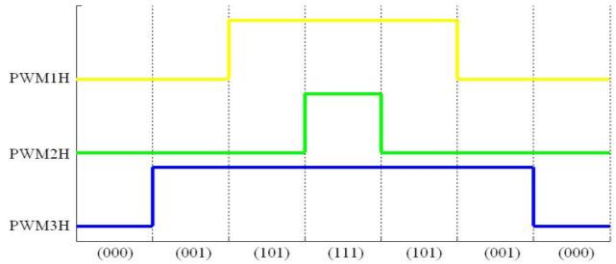

Figure 26. Third changes in voltage combination.

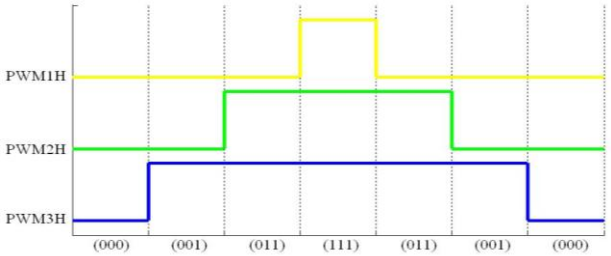

Figure 27. Fourth changes in voltage combination.

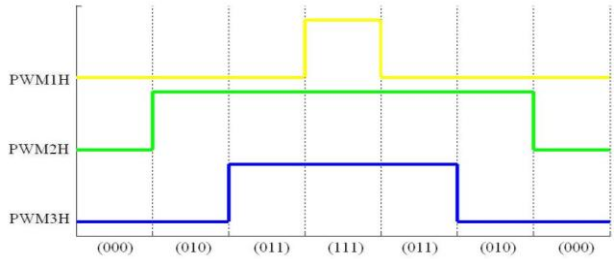

Figure 28. Fifth changes in voltage combination.

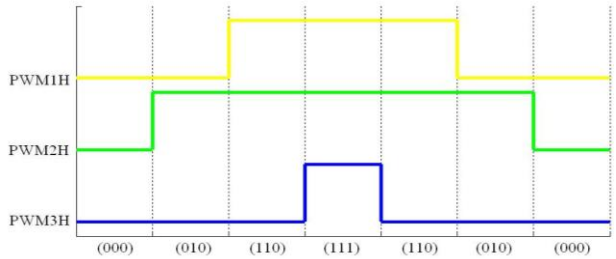

Figure 29. Sixth changes diagram in voltage combinations.

IV. EXPERIMENTAL RESULTS AND ANALYSIS

Sine wave generated by sine width modulation from dsPIC30F4011 is used to drive the motor. Therefore, the transistor can send respective order switching signal, shown in Table III. The voltage state of "1" indicates the upper arm switch turned off and the lower arm switched off; "0"indicates the switch off at the upper arm and lower arm switch is turned on. This produces six combinations.

ISBN: 978-988-19252-7-5
ISSN: 2078-0958 (Print); ISSN: 2078-0966 (Online)

TABLE Ⅲ
VOLTAGE COMBINATIONS

	Voltage state						
1	000	100	110	111	110	100	000
2	000	100	101	111	101	100	000
3	000	001	101	111	101	001	000
4	000	001	011	111	011	001	000
5	000	010	011	111	011	010	000
6	000	010	110	111	110	010	000

In actual test results from Figures 30 to 35, we see that the start and end of the voltage states are 000 (all upper arm switches are turned off), and each combination must have 111 (upper arm switch is turned on) in all the voltage states. It means that each time has only one change so that switching times are reduced significantly.

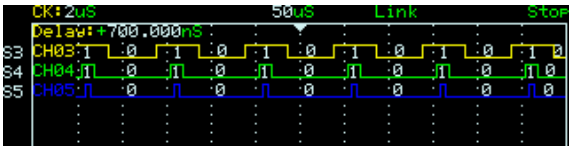

Figure 30. First voltage combination in the actual test results.

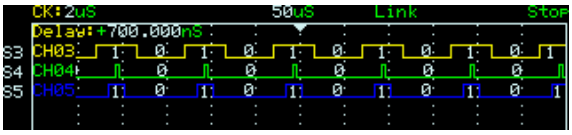

Figure 31. Second voltage combination in the actual test results.

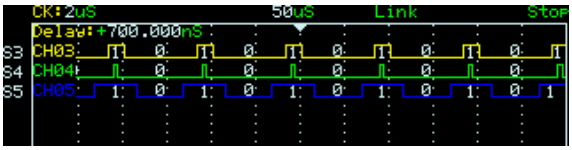

Figure 32. Third voltage combination in the actual test results.

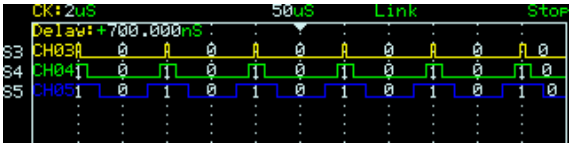

Figure 33. Fourth voltage combination in the actual test results.

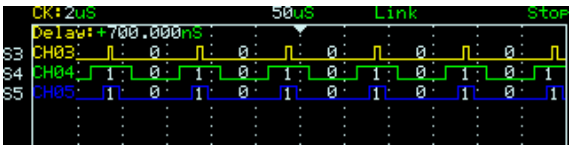

Figure 34. Fifth voltage combination in the actual test results.

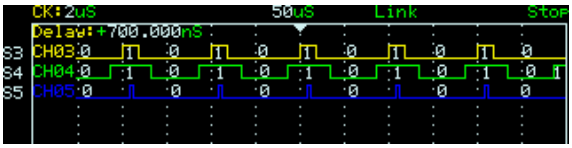

Figure 35. Sixth voltage combination in the actual test results.

The QEI interrupt dsPIC30F4011 chip is specifically used as an incremental encoder interface, and POSCNT is used as a count register for motor positive and reverse rotation.

V. CONCLUSION

Based on the characteristics of AC motor, the speed of rotating magnetic field is controlled by the stator voltage frequency, and thus the motor speed is changed by the rotational speed of rotator. In this study, we used digital signal processor dsPIC30F4011 as the system controller core with C language programming. The proposed controller can provide appropriate SPWM signals for the inverter switching, motion commands and position feedback signal using IGBT. At a time, only one switch is activated and the power loss due to switching frequency is reduced. Both simulation and experimental results have verified the effectiveness of the proposed system in term of robustness and stability.

REFERENCES

[1] J. P. Karunadasa, A. C. Renfrew, "A flexible fast digital controller for a brushless DC motor", *The Fourth International Conference on Power Electronics and Variable-Speed Drives*, pp. 429-434, 1990.
[2] W. H. Sakmann, "A brushless DC motor controlled by a microprocessor with examples for a three-phase motor", *IEEE Transactions on Industrial Electronics*, vol. 34, pp. 339-344, 1987.
[3] A. Murray, P. Kettle, and F. Moynihan, "Advances in brushless motor control", *American Control Conference*, vol. 6, pp. 3985-3989, 1997.
[4] G. Pellegrino, R. I. Bojoi, P. Guglielmi, "Unified direct-flux vector control for AC motor drives," *IEEE Transactions on Industry Applications*, vol. 47, pp. 2093-2102, Sept.-Oct. 2011.
[5] A. Sayed-Ahmed, N. A. O. Demerdash, "Fault-tolerant operation of delta-connected scalar- and vector-controlled AC motor drives," *IEEE Transactions on Power Electronics*, vol. 27, pp. 3040-3049, June 2012.
[6] L. -H. Hung, "Brushless Permanent Magnet Motor, Analysis and Testing, " *Journal of mechanics*, vol. 377, Yeh Yin Press, 2006.
[7] M. A. Chaudhari, H. M. Suryawanshi, M. M. Renge, "A three-phase unity power factor front-end rectifier for AC motor drive," *IET Power Electronics*, vol. 5, pp. 1-10, January 2012.
[8] S. -H. Wang, "Brushless DC motor drive with FPGA-based design and production," Southern Taiwan University of Science and Technology, Master's thesis, 2004.
[9] G. Liu and W. G. Dunford, "Comparison of sinusoidal excitation and trapezoidal excitation of a brushless permanent magnet motor," *IEEE The Fourth International Conference on Power Electronics and Variable-Speed Drives*, pp. 446-451, 1998.
[10] J. B. Lee, J. H. Choi, J. K. Chung, and J. H. Lim, "Design and implementation of integrated drive circuit for a small BLDC motor," *2003 ICEMS Electrical Machines and Systems*, 2003.
[11] H. Sira-Ramirez, F. Gonzalez-Montanez, J. A. Cortes-Romero, A. Luviano-Juarez, "A robust linear field-oriented voltage control for the induction motor: experimental results," *IEEE Transactions on Industrial Electronics*, vol.60, pp. 3025-3033, August 2013.
[12] O. Wallmark, S. Lundberg, M. Bongiorno, "Input admittance expressions for field-oriented controlled salient PMSM drives, " *IEEE Transactions on* Power Electronics, vol. 27, pp. 1514-1520, March 2012.
[13] A. Iqbal and S. Moinuddin, "Comprehensive relationship between carrier-based PWM and space vector PWM in a five-phase VSI," *IEEE Transactions on Power Electronics*, vol. 24, pp. 2379-2390, 2009.
[14] Oscar López, Drazen Dujic, Martin Jones, Francisco D. Freijedo, Jesús Doval-Gandoy, and Emil Levi, "Multidimensional two-level multiphase space vector PWM algorithm and its comparison with multi frequency space vector PWM method," *IEEE Transactions on Industrial Electronics*, vol. 58, pp. 465-475, 2011.
[15] Luca Bascetta, Gianantonio Magnani, Paolo Rocco and Andrea Maria Zanchettin, "Performance limitations in field-oriented control for asynchronous machines with low resolution position sensing," *IEEE Transactions on Control Systems Technology*, vol. 18, pp. 559-573, 2010.
[16] A. K. Jain and V. T. Ranganathan, "Modeling and field oriented control of salient pole wound field synchronous machine in stator flux coordinates," *IEEE Transactions on Industrial Electronics*, vol. 58, pp.960-970, 2011.
[17] W. Kim, C. Yang, and C. C. Chung, "Design and implementation of simple field-oriented control for permanent magnet stepper motors without DQ transformation," *IEEE Transactions on Magnetics*, vol. 47, pp. 4231-4234, 2011.
[18] A. M. Bazzi, A. Dominguez-Garcia and P. T. Krein, "Markov reliability modeling for induction motor drives under field-oriented control," *IEEE Transactions on Power Electronics*, vol. 27, pp. 534-546, February 2012.
[19] O. S. Ebrahim, M. F. Salem, P. K. Jain, M. A. Badr, "Application of linear quadratic regulator theory to the stator field-oriented control of induction motors," *IET Electrical Power Applications*, vol. 4, pp. 637-646, September 2010.

ISBN: 978-988-19252-7-5
ISSN: 2078-0958 (Print); ISSN: 2078-0966 (Online)